


Combo-PON OLT Transceiver Using Photonic Integration Technology

Hongqing Ding, Zeru Wu, Yuanfeng Mao, Xu Wang, Qihong Wu, Yuanbing Cheng, Yanbo Li, Tianhai Chang, and Ruiqiang Ji 

Abstract—In this work, a prototype of 10G Combo-PON OLT transceiver based on photonic integrated circuits (PIC) is proposed and demonstrated. Key optical components for Combo-PON OLT transceiver, including high-power DFB laser, micro-ring modulator and WDM, have been developed and validated. The Combo-PON OLT transceiver integrated four XGS-PON/GPON ports and all ports comply with I-TUT G.984.2 Class C+ standard. The advantages and disadvantages of PIC in PON application are analyzed. The analysis shows that PIC can also provide a cost and power-efficient way to implement the next generation PON transceiver for high density PON ports.

Index Terms—Passive optical network, photonic integration, optical transceiver.

I. INTRODUCTION

THE passive optical network (PON) is one of the most competitive network for global operators, due to its advantages of high bandwidth, stability, simplified architecture and long-term development [1]. PON with a point-to-multipoint network architecture has been successfully deployed on a large scale for decades with upstream and downstream access bandwidth of around 1.25 and 2.5 GHz, respectively. With the rapid development of the high traffic video services such as 4K/8K, augmented reality (AR)/virtual reality (VR) and cloud computing, and explosive growth of user requirement for bandwidth, the optical access network enters the stage of mass construction of 10G PON. However, smooth network evolution needs to meet the requirements of reuse of existing optical distribution network (ODN) and forward compatibility of legacy ONUs, which imposes higher requirements for the PON technology.

Therefore, Combo-PON is proposed to evolve and migrate from GPON to 10G PON, as shown in Fig. 1. In Combo-PON, Combo-PON cards are used to replace the existing GPON cards at the optical line terminal (OLT) side. Optical transceiver

Manuscript received 5 August 2022; revised 1 September 2022; accepted 7 September 2022. Date of publication 12 September 2022; date of current version 26 September 2022. (Corresponding author: Ruiqiang Ji.)

Hongqing Ding is with the China Mobile Communications Group Company, Ltd., Beijing 100007, China (e-mail: dinghongqing@chinamobile.com).

Zeru Wu, Qihong Wu, Yanbo Li, Tianhai Chang, and Ruiqiang Ji are with the Optical Research Department, Huawei Technologies Company, Ltd., Dongguan 523000, China (e-mail: wuzeru@huawei.com; wuqihong@huawei.com; li.yanbo@huawei.com; changtianhai@huawei.com; jiruiqiang@huawei.com).

Yuanfeng Mao, Xu Wang, and Yuanbing Cheng are with the Optical Research Department, Huawei Technologies Company, Ltd., Wuhan 430000, China (e-mail: maoyuanfeng@huawei.com; wangxu108@huawei.com; chengyuanbing@huawei.com).

Digital Object Identifier 10.1109/JPHOT.2022.3205783

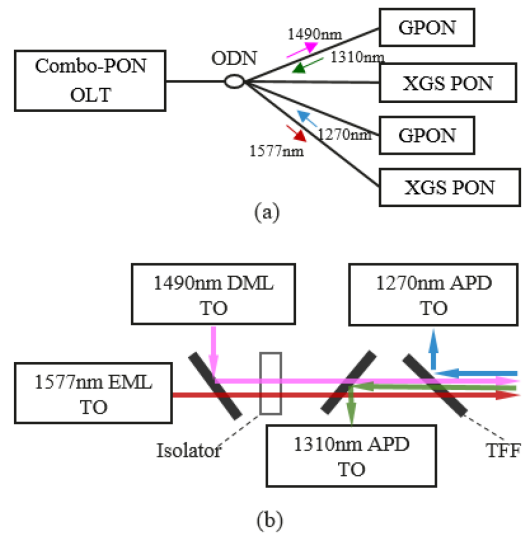


Fig. 1. (a) Concept illustration of Combo-PON network. (b) Schematic diagram of OSA based on TO-can active devices and free space optical components used in Combo-PON OLT transceiver (Lines with arrows represent optical signals, and different colors represent different wavelengths).

modules on the board of Combo-PON cards combine GPON, 10G PON and wavelength-division multiplexer (WDM) optical modules into one to reuse the ODN. This module can connect with XGS-PON and GPON optical network units (ONUs) over a single fiber via wavelength division multiplexing. A typical schematic diagram of the optical sub-assembly (OSA) in Combo-PON OLT transceiver is shown in Fig. 1(b). It consists of four TO pre-packaged active devices and some free-space optical components including optical collimators, optical isolators and thin film filters (TFF). Compared with a single GPON or XGS-PON OSA, Combo-PON OSA has a larger size and needs more complex packaging processes. Moreover, the power consumption is nearly doubled for Combo-PON transceiver. Therefore, it is extremely challenging to implement and maintain the high density PON ports in a Combo-PON card using such free space coupling and discrete packaging scheme for the fabrication of Combo-PON transceiver. Optical integration technology may be a good solution for this complex transceiver.

In fact, various optical integration technologies have been developed for PON devices. Hoya used a so-called Surface Mounted Photonics technology [2], OneChip Photonics developed InP PIC for GPON application [3], and Google tried to

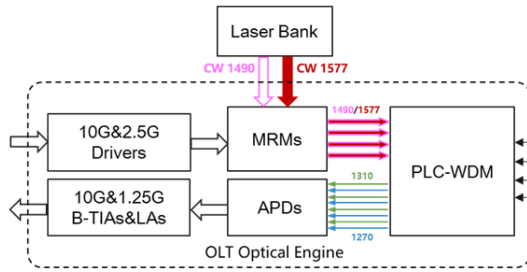


Fig. 2. The proposed architecture of Combo-PON OLT transceiver. It consists of LB pluggable module and on-board OE module.

use silicon photonics for WDM PON devices [4]. The attempt of optical integration technology has yielded some remarkable results, which also gave us a deeper understanding of the position of the integrated optical devices in the optical access network. For GPON application, the fabrication of optical transceivers is not so challenging that both hybrid integration of active devices [2] and InP PIC [3] cannot enhance the competitiveness of PON transceivers. Currently, optical integration technologies are mature enough for commercial use [5]. We believe it will deliver significant performance and cost benefits to the optical transceivers for both 10G PON and next generation PON.

In this paper, we propose and demonstrate a 4-channel 10G Combo-PON OLT transceiver with a new architecture for high density PON ports using optical integration technologies. The transceiver includes one pluggable laser bank and one optical engine. In the laser bank, there are 4-channel 1577 nm single-mode optical output and 4-channel 1490 nm single-mode optical output, where the output power of each channel is more than 16 dBm. An on-board optical engine is also included to modulate the continuous-wave light from the laser bank and couple the optical signals into the optical fibers. It is also used to demultiplex and detect the upstream signals from both GPON and XGS-PON ONUs and avoid crosstalk between each channels of both downstream and upstream signals. Experimental results show that the average optical power of 1490-nm and 1577-nm transmitter per channel is larger than 3 dBm and 5 dBm, respectively. The receiver sensitivity per channel is -37.6 dBm and -30 dBm for 1.25-Gbps and 10-Gbps bit rate, respectively. The 4-channel Combo-PON OLT transceiver can support C+ application, simultaneously.

II. TRANSCEIVER ARCHITECTURE AND FABRICATION

The proposed architecture of Combo-PON OLT transceiver including one pluggable laser bank and one optical engine (OE) is shown in Fig. 2. The concept of laser ‘bank’, which refers that the optical power from each laser channel can be shared by multiple silicon photonic (SiPh) modulators in OE, is a promising way to reduce the cost of the transceiver. Meanwhile, thermal management of the transceiver becomes easy, since the hottest banks of lasers are externally connected with the OE and individually packaged. The work temperature of the laser banks can be efficiently controlled by a powerful TEC. Another advantage of this architecture is that the light generation and signal modulation are decoupled, which means that

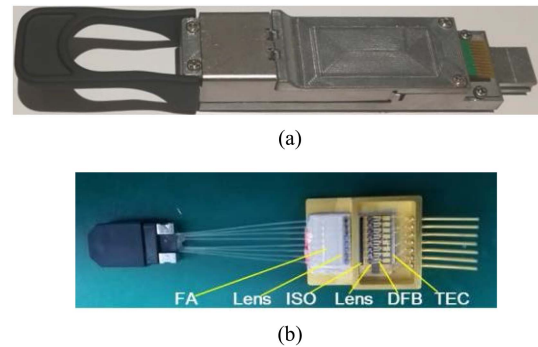


Fig. 3. (a) Images of the pluggable LB module and (b) the details inside the LB box.

the performance of lasers and modulators can be optimized independently. Therefore, a higher power and more efficient laser can be designed [6]. In the laser bank, there are 4-channel 1577 nm single-mode optical output and 4-channel 1490 nm single-mode optical output.

An on-board optical engine is also included for light modulation and detection. In the OE, silicon micro-ring modulators (MRM) are used for both 1577 nm and 1490 nm downstream light modulation. In addition to MRM, normal incidence APDs and TIAs are also included as upstream receivers. Eight modulators and eight receivers are optically connected by a polarization independent PLC-based WDM with low insertion loss. In one channel of the transceiver, two pairs of upstream and downstream signals (1270/1577, 1310/1490 nm) are coupled to single-mode fiber through one of the four WDM output waveguides. It is clear that core devices in the OE are fabricated by photonic integration technology with small footprints. This design enables the multi-channel integration and the independent evolution to the monolithically integrated optical chip.

For maintainability, LB is packaged as a pluggable module assembled from pre-packaged lasers, as shown in Fig. 3. Unlike a traditional pluggable optical transceiver, the optical output connector of LB is located at the same side of its electrical connector. An integrated optical and electrical adaptor is mounted on a PCB. When the LB module is inserted into the host PCB by means of integrated adaptors, optical and electrical connections to the on-board SiPh chip are formed simultaneously. More details of LB module and adaptor can be found in reference [7]. Pre-packaged DFB lasers are shown in Fig. 3(b). It is delivered in a hermetic box package with a TEC for temperature control to avoid wavelength drifts. Optical isolator with isolation ratio of around 30 dB are used here to avoid back reflection of light into the DFB lasers to guarantee the transmission performance. Dual-lens coupling scheme is adopted to provide high coupling efficiency with high coupling tolerance. The external packaged LB module has advantages of lower optical source cost, enhanced maintainability with energy-efficient thermal management.

Fig. 4(a) shows the structure of OSA used in the on-board OE module. It consists of one SiPh MRM chip with eight MRMs, eight APDs and one WDM chip with pigtail fiber. CW light from LB passes through the PLC chip before being launched into the modulator chip. As the core component, the

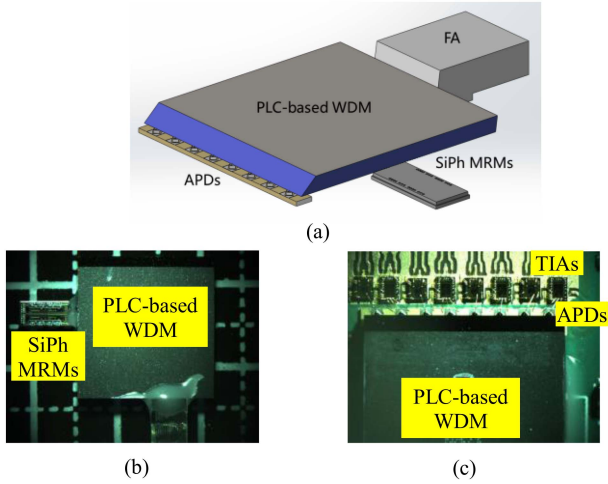


Fig. 4. (a) Schematic diagram of OSA in OE module. The coupling details among PLC-based WDM and (b) SiPh MRM chip and (c) APD array.

TABLE I
TEST RESULTS OF LB MODULE

Channel #	Wavelength (nm)	Optical power (dBm)
CH1 L-band	1577.2	16.17
CH2 L-band	1578.8	16.46
CH3 L-band	1577.1	16.16
CH4 L-band	1578.5	16.20
CH1 S-band	1488.8	12.96
CH2 S-band	1490.3	16.72
CH3 S-band	1493.3	16.12
CH4 S-band	1491.1	14.63

WDM chip uses the multi-stage cascaded MZI filters with a high wavelength isolation ratio to multiplex and demultiplex four independent wavelength (1270/1310/1490/1577 nm). It should be noted that a cascaded MZI structure offers negligible insertion loss, scalability, and high design freedom [8]. For high performance WDM, the waveguide dispersion including wavelength-dependent coupling ratio variation and phase errors should be carefully considered. The WDM was fabricated on a polarization-insensitive low-index-contrast PLC platform, which is widely used for optical distribution network in PON. The interconnection between the WDM chip and MRM chip is realized through a chip-to-chip butt coupling scheme. All components are mounted directly on the PCB.

III. TRANSCEIVER CHARACTERIZATION

A. Laser Bank

Table I shows the test results of one LB module with eight DFB lasers inside. To reduce the power consumption of the module, the working temperature of DFB lasers is set to 60° C to minimize the power consumption of TEC. The total power consumption of LB module is about 6.9 W. The emission wavelengths of LB comply with 10G Combo-PON standard. The DFB laser with a wavelength of 1577 nm has an output power of more than

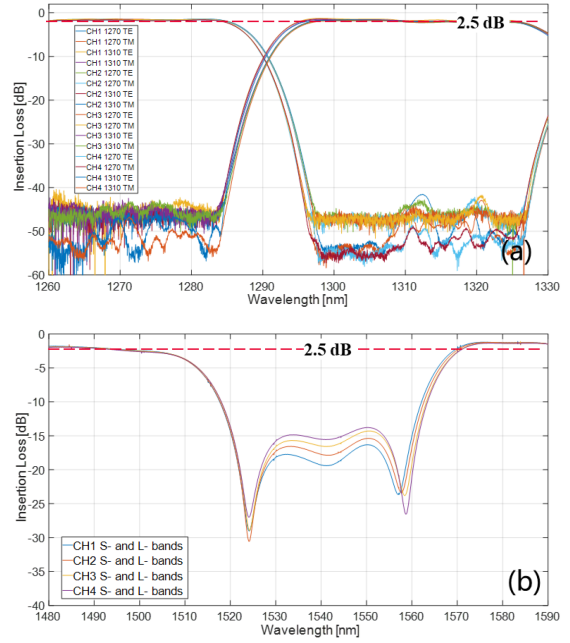


Fig. 5. Transmission spectrum of the on-chip WDM filters in (a) S- and L-band for downstream wavelengths combining and (b) O-band for upstream wavelengths separation.

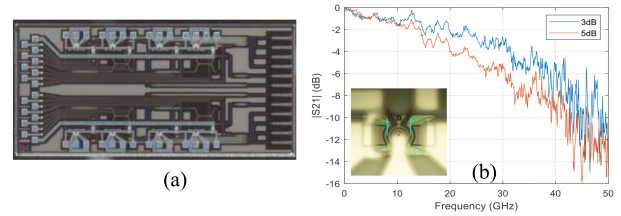


Fig. 6. (a) The image of SiPh MRM chip. (b) $|S_{21}|$ curves of MRM under different working points.

16 dBm per channel, whereas the DFB laser with a wavelength of 1490 nm in the LB has an output power of around 14 dBm per channel, except for CH1. The lower output power in CH1 is induced by a bad coupling between DFB laser and pigtail fiber. The total optical insertion loss for the downstream signal includes coupling loss between LB and optical engine, coupling loss between optical engine and single-mode fiber as well as intrinsic on-chip loss in each component is around 11 dB for both 1490 nm and 1577 nm in the transceiver module. Therefore, the average output optical power of the transceiver per channel is larger than 3 dBm and 5 dBm for 1490-nm and 1577-nm, respectively.

B. Optical Engine

The performance of PLC WDM chip was characterized by a wavelength scanning system including a tunable laser, polarization controllers and optical power meter. Fig. 5 shows the transmission spectra of the WDM device. Due to a delicate design of the cascaded MZI filter and the low-birefringence square waveguide structure, a polarization-insensitive and flat-top response for all four wavelengths are demonstrated. The total insertion loss for both O- and L-band, including WDM on-chip

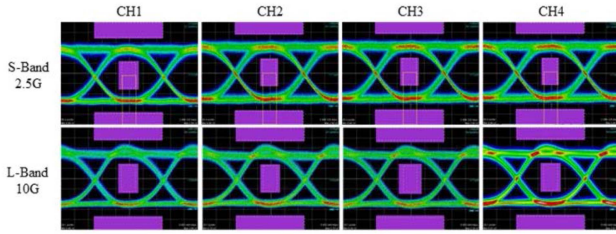


Fig. 7. The back-to-back optical eyes. 2.5 Gbps and 10 Gbps optical eyes with ER of higher than 8.2 dB.

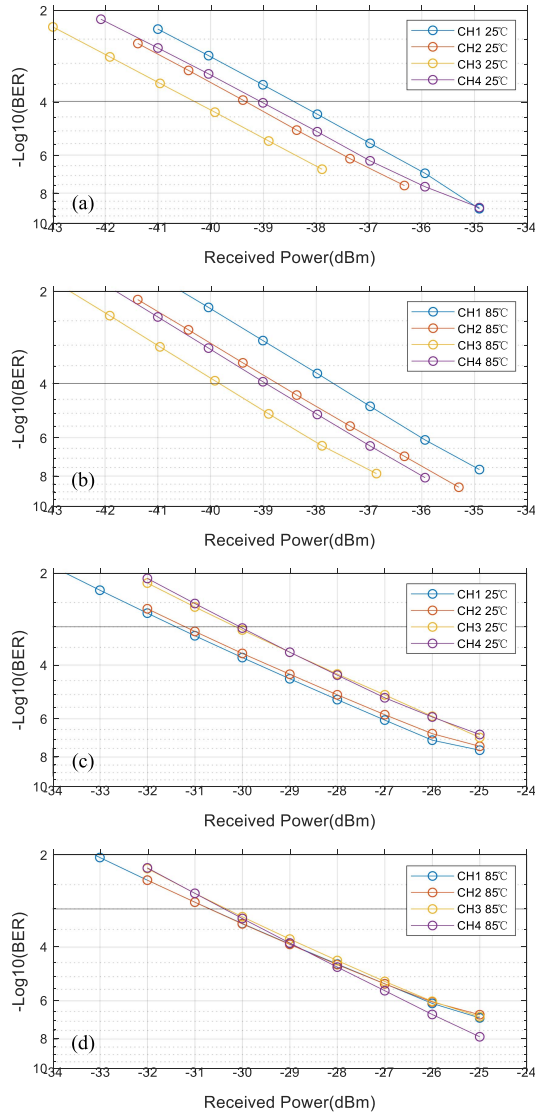


Fig. 8. 1.25-Gbps receiver sensitivity at (a) 25 °C and (b) 85 °C, 1310 nm. 10-Gbps receiver sensitivity at (c) 25 °C and (d) 85 °C, 1270 nm.

loss and coupling losses between two fiber-chip interfaces, are around 2.5 dB. The relatively large insertion loss in the S band is caused by a slight deviation in the central wavelength of the downstream multiplexer, which can be easily improved in the future iterations. Most importantly, upstream wavelength demultiplexing is successfully demonstrated with a crosstalk of less than -30 dB.

TABLE II
COMPARISON OF THIS WORK WITH TFF-BASED WDM

	On-chip WDM (This work)	TFF-based WDM
Insertion loss (dB)	1260-1280 nm	<2.2
	1300-1320 nm	<2.4
	1480-1500 nm	<2.8
	1575-1580 nm	<2.1
Ripple (dB)	<0.5	<0.5
Return loss (dB)	>40	>45
Polarization dependent loss (dB)	<0.2	<0.2
Crosstalk between upstream channels	>35	>30

Table II shows the performance comparison between the on-chip WDM filter and the typical built-in TFF in the optical module. Although the WDM fabricated in this work has excellent performance, the gap of insertion loss is still >1 dB, mainly due to high coupling loss, which applies to almost all integrated photonic chips. Nonetheless, high-performance on-chip WDM remain attractive for Combo-PON due to their advantage of scalability and ease of packaging. Besides, the on-chip WDM solutions provide the opportunity for monolithic integration of modulators and APDs, which can be more cost-effective compared to free-space optics packaging.

Fig. 6(a) shows an image of a fabricated SiPh MRM chip comprising four 1490 nm MRMs, four 1577 nm MRMs and four 1490 nm/1577 nm multiplexer based on directional couplers. Compared with DML and EML for light modulation, SiPh modulators has smaller chirps. Moreover, the design and fabrication of SiPh modulators is very flexible. Modulators with different bit-rate and operating wavelength can be fabricated on a single chip without extra efforts. For SiPh modulators, MRM has smaller footprint and lower power consumption than MZ modulator [9], [10]. Therefore, MRM are more suitable to PON application. Because MRM is temperature sensitive and operates over a narrow wavelength range, a closed-loop control circuit with fine wavelength locking and TEC is used here. Fig. 6(b) shows the measured E/O responses of MRM at different working points. The 3 dB bandwidth is 15 GHz at the -5 dB working point. The measured back-to-back 2.5G and 10G optical eye diagrams for all four channels are shown in Fig. 7, with extinction ratios larger than 8.2 dB. Here EML drivers are used for MRMs due to the lack for commercial MRM drivers. The overshoots in the 10 Gbps eye patterns can be eliminated with better impedance matching between MRMs and drivers. Moreover, the eye patterns can be further improved with simpler but efficient customized driver directly driven by a CMOS inverter [11].

The receiver includes eight normal incident APDs, four 10G and four 1.25G commercial TIAs. The normal incident structure of APD was used here to avoid polarization problems [12]. The coupling loss between WDM chip and APD is less than 0.5 dB. Fig. 8 shows the back-to-back BER test results of all four channels at 25 °C and 85 °C, respectively. We can find that the highest sensitivities are -40.3 dBm and -31.4 dBm for 1.25 Gbps and

10 Gbps at 25 °C, respectively. The sensitivity degradation is about 1 dB at 85 °C, which is mainly caused by the high dark current and the deterioration of the coupling insertion loss between the APD and PLC WDM at a high temperature. The sensitivity difference of the four channels is due to the difference among the APD chips as well as the coupling insertion loss caused by the non-uniformity of the APD assembly. Finally, the receive sensitivity at 1.25 Gbps and 10 Gbps are -37.6 dBm and -30 dBm, respectively, for all four channels. As stated previously, the average output optical power of the transceiver per channel is larger than 3 dBm and 5 dBm for 1490-nm and 1577-nm, respectively. Therefore, it proves that the 4-channel Combo-PON OLT transceiver is capable of supporting Class C+ applications.

IV. CONCLUSION

We proposed and reported a prototype of 4-channel 10G Combo-PON OLT transceivers for high density PON ports based on PIC. The transceiver includes a pluggable laser bank and one optical engine. The laser bank with high power DFB lasers is fabricated by III-V photonic integration technology, while the optical engine with MRMs and WDMs are fabricated by SiPh and PLC integrated circuits, respectively. Experimental results show that the Combo-PON OLT transceiver can support XGS-PON/GPON OLT C+ application, simultaneously. The performance of the transceivers can be further improved with dedicated device optimization, improvement of photonic integration technology and packaging. It proves that PIC can also provide a power-efficient way to implement the next generation PON transceiver for high density PON ports. Although PON is a cost-sensitive solution for offering wide communication services, the market size of PON device is expected to grow rapidly over the forecast period. The scale effect will lower the

device cost, but also speeds up the maturity of the new photonic integrated technology.

REFERENCES

- [1] "The fifth generation fixed network (F5G): Bringing fibre to everywhere and everything," ETSI White Paper #41, Sep. 2020. [Online]. Available: https://www.etsi.org/images/files/ETSIWhitePapers/etsi_wp_41_FSG_ed1.pdf
- [2] H. Blauvelt et al., "High performance planar lightwave circuit triplexer with passive optical assembly," in *Proc. Opt. Fiber Commun. Conf.*, 2005, Paper OThU7.
- [3] V. Tolstikhin, "Regrowth-free multi-guide vertical integration in InP for optical communications," in *Proc. 23rd Int. Conf. Indium Phosphide Related Mater.*, 2011, pp. 1–4.
- [4] R. Urata, H. Liu, C. Lam, P. Dashti, and C. Johnson, "Silicon photonics for optical access networks," in *Proc. 9th Int. Conf. Group IV Photon.*, 2012, pp. 207–209.
- [5] H. Yu et al., "100 Gbps CWDM4 silicon photonics transmitter for 5G applications," in *Proc. Opt. Fiber Commun. Conf.*, 2019, Paper W3E.4.
- [6] Y. Mao, Y. Cheng, B. Xu, R. Ji, and Y. Li, "Record-high power 1.55- μ m distributed feedback laser diodes for optical communication," in *Proc. Opt. Fiber Commun. Conf.*, 2021, Paper W1B.7.
- [7] B. Xu, R. Li, Y. Li, and X. Song, "High power external pluggable laser bank with simultaneous single mode optical & electrical connection," in *Proc. Opt. Fiber Commun. Conf.*, 2020, pp. 1–3.
- [8] T. Lee, D. Lee, and Y. Chung, "Design and simulation of fabrication-error-tolerant triplexer based on cascaded Mach-Zehnder interferometers," *IEEE Photon. Technol. Lett.*, vol. 20, no. 1, pp. 33–35, Jan. 2008, doi: [10.1109/LPT.2007.910758](https://doi.org/10.1109/LPT.2007.910758).
- [9] X. Xiao et al., "25 Gbit/s silicon microring modulator based on misalignment-tolerant interleaved PN junctions," *Opt. Exp.*, vol. 20, no. 3, pp. 2507–2515, Jan. 2012, doi: [10.1364/OE.20.002507](https://doi.org/10.1364/OE.20.002507).
- [10] Y. Zhang et al., "200 Gbit/s optical PAM4 modulation based on silicon microring modulator," in *Proc. Eur. Conf. Opt. Commun.*, 2020, pp. 1–4.
- [11] H. Li et al., "A 25 Gb/s, 4.4 V-swing, AC-coupled ring modulator-based WDM transmitter with wavelength stabilization in 65 nm CMOS," *IEEE J. Solid-State Circuits*, vol. 50, no. 12, pp. 3145–3159, Dec. 2015, doi: [10.1109/JSSC.2015.2470524](https://doi.org/10.1109/JSSC.2015.2470524).
- [12] L. Liu et al., "Low-cost hybrid integrated 4 \times 25 GBaud PAM-4 CWDM ROSA with a PLC-based arrayed waveguide grating demultiplexer," *Photon. Res.*, vol. 7, no. 7, pp. 722–727, Jun. 2019, doi: [10.1364/PRJ.7.000722](https://doi.org/10.1364/PRJ.7.000722).